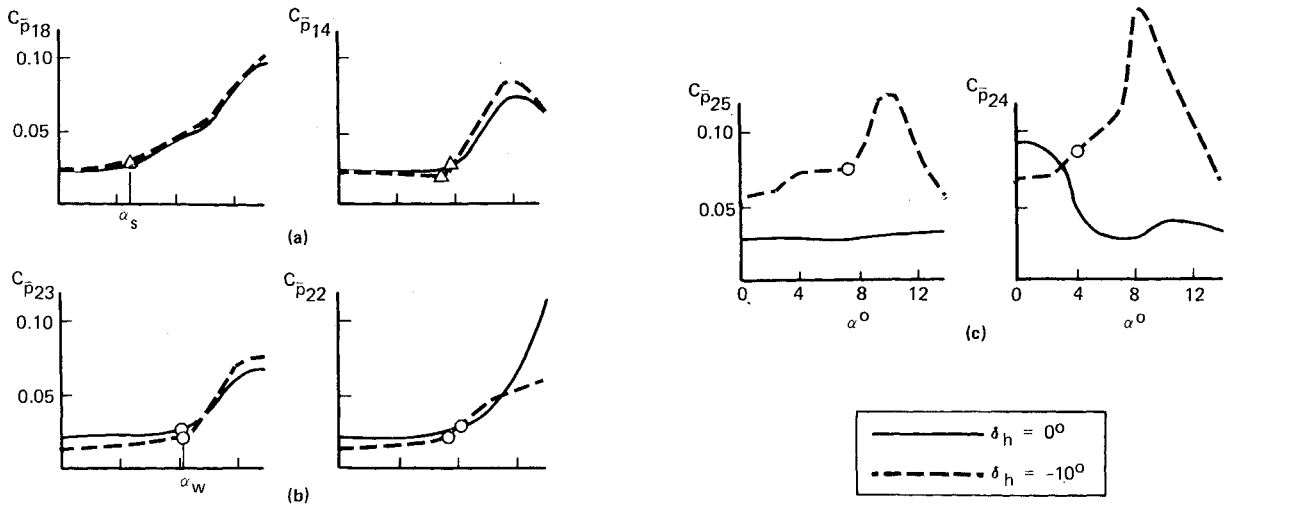

Fig. 4 Dynamic pressure coefficient comparison including tail deflection effect, $\delta_\psi/\delta_f = 5/12$ deg, $M = 0.75$, $Q = 15.6$ kN/m^2, $Re = 2.48 \times 10^6$.

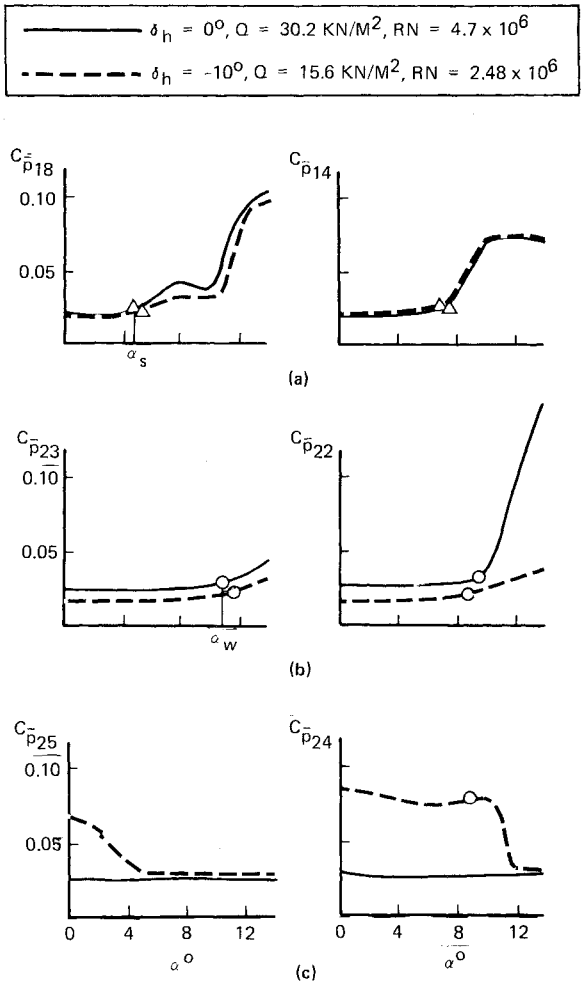

Fig. 5 Dynamic pressure coefficient comparison including tail deflection effect, $\delta_n/\delta_f = 0/0$ deg, $M = 0.75$.

buffet is encountered. The data presented in this note serve to demonstrate a number of contributing factors that affect the tail dynamic pressures in the transonic regime.

Acknowledgment

The test data reported in this note were acquired under NASA Ames Research Center Contract NAS2-8734, "F-5A Wind Tunnel Buffet Investigation." Mr. Charles Coe was the NASA program monitor.

References

[1] Hwang, C. and Pi, W.S., "Investigation of Steady and Fluctuating Pressures Associated with the Transonic Buffeting and Wing Rock of a One-Seventh Scale Model of the F-5A Aircraft," NASA Contract Rept., 3061, Nov. 1978.

[2] Hwang, C. and Pi, W.S., "Some Observations on the Mechanism of Aircraft Wing Rock," presented as Paper 78-1456 at the AIAA Aircraft Systems and Technology Meeting, Los Angeles, Calif., Aug. 21-23, 1978.

Transonic Shock-Boundary-Layer Interactions in Cryogenic Wind Tunnels

G.R. Inger*
Virginia Polytechnic Institute and State University, Blacksburg, Va.

Introduction

SINCE the transonic aerodynamics of missiles and aircraft can be significantly influenced by shock wave – boundary layer interaction effects, these effects should be adequately simulated in cryogenic high Reynolds number wind tunnel experiments. In addition to flight Mach and Reynolds numbers which are by design simulated in such facilities,[1] there are four other similitude parameters which may not be duplicated owing to the very low temperature-high pressure working fluid involved: wall to total temperature ratio T_w/T_t, specific heat ratio γ, viscosity temperature exponent ω, and Prandtl number Pr. The first is deemed especially important since in some proposed short duration cryogenic transonic wind tunnels the model is at a much higher temperature than

Presented as Paper 78-808 at the AIAA 10th Aerodynamic Testing Conference, San Diego, Calif., April 1978.

Index categories: Boundary Layers – Turbulent; Shock Waves; Transonic Flow.

*Professor, Dept. of Aerospace and Ocean Engineering. Associate Fellow AIAA.

T_t during the test. Moreover, the γ of cryogenic nitrogen flow can be larger (1.5-1.8) than air[2] and thus may influence the interaction effects. Lower γ's are also of interest in heavy gas (Freon 12) facilities.[3] This note describes the results of extending an approximate nonasymptotic theory of weak normal shock nonseparating turbulent boundary layer interaction to include these effects of heat transfer and arbitrary γ, ω and Pr.

Theoretical Model

Consider an isobaric turbulent boundary-layer Mach number profile $M_0(y)$ slightly perturbed by an impinging weak normal shock. For nonseparating interactions (local Mach number $M \lesssim 1.3$) in the Reynolds number range $Re_L \sim 0(10^6)$ we employ a nonasymptotic viscous disturbance flow model patterned after the Lighthill-Stratford double-deck approach which has proven very successful in treating turbulent boundary-layer response to strong rapid adverse pressure gradients[4,5] and which is supported by a large body of transonic and supersonic interaction data and a general theoretical study.[6] The resulting flow model (Fig. 1) consists of an inviscid boundary value problem surrounding a shock discontinuity and underlaid by a thin viscous disturbance sublayer that contains the upstream influence and skin friction perturbation. An approximate analytic solution is further achieved by assuming small linearized disturbances ahead of and behind the nonlinear shock jump plus neglect of the detailed shock structure within the boundary layer, which give accurate predictions for all the properties of engineering interest when $M_1 \gtrsim 1.05$.[7,8] As described in detail elsewhere,[7] the resulting equations can be solved by operational methods with an arbitrary γ, yielding the interactive pressure rise and displacement thickness growth and a recently-extended skin friction solution[8] that now includes the region downstream as well as upstream of the shock foot and nonlinear incipient-separation effects.

It can be shown[9] that moderate heat transfer does not introduce any new terms in either the inviscid or viscous disturbance equations; it significantly influences the interaction only through the undisturbed $M_0(y)$, skin friction C_{f_0} and boundary layer thickness δ_0. The input $M_0(y)$ is based on an accurate flat plate turbulent eddy viscosity model with arbitrary ω that is well-suited for interation studies[7,8]; it uses a modified Crocco-integral $T(y)$ with arbitrary heat transfer, recovery factor $r \approx P_r^{1/3}$ and γ. For preliminary engineering purposes note that we have used a simplified real gas model involving constant thermodynamic (γ) and transport (ω, Pr) properties; should their effect be significant, it is understood that a more detailed treatment of these properties might be necessary.

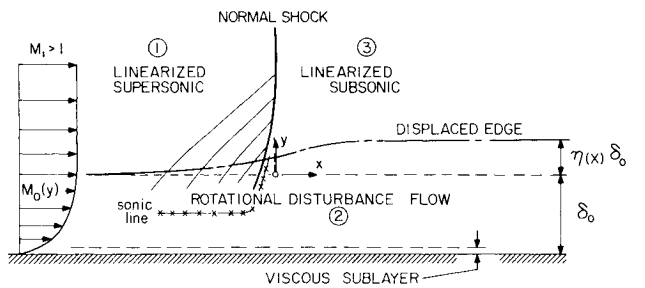

Fig. 1 Normal shock-turbulent boundary-layer interaction flow model (schematic).

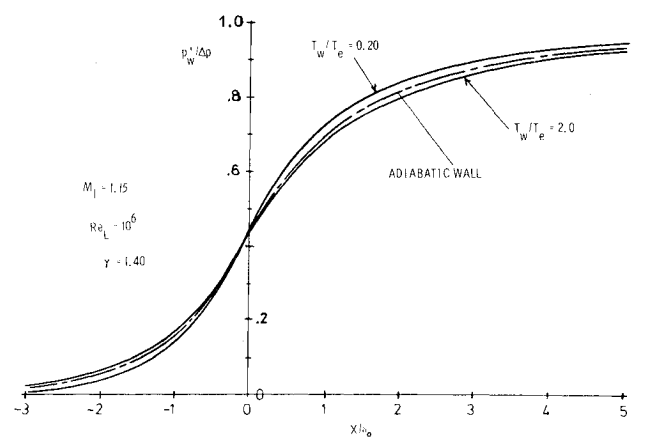

Fig. 2 Wall temperature effect on surface pressure distribution.

Discussion of Results

To cover various facilities with different gases and/or thermal histories (ranging from fan-driven or blow-down to short duration Ludwieg tubes), a wide range of the parameters was studied[10]; the following are typical results.

The predicted T_w effect on the wall interaction pressure distribution, shown in Fig. 2, was weak as expected (this was true over a range of M_1 and Re_L). Increasing T_w slightly increases the nondimensional upstream influence distance and lowers the downstream pressure. The reduction of upstream influence is thus proportional to that of δ_0.

The interactive displacement thickness is of practical interest since this often has a significant back-effect on the inviscid flow and shock position on an airfoil or in channel flows. Figure 3 illustrates the expected reduction that occurs with increased cooling; the influence of a hot wall $T_w > T_t$ is increasingly significant at lower Re_L. The corresponding effect on $C_f(x)$ is also important because it alters the downstream boundary-layer growth and possible separation. Since T_w influences C_{f_0}, the relative effect on its interactive decrement is shown in Fig. 4a as the ratio $C_f(x)/C_{f_0}$. Owing to the interaction-induced adverse pressure gradient, C_f/C_{f_0} typically decreases downstream toward the shock with a minimum occurring slightly behind it, followed by a subsequent gradual rise further downstream. It is seen that wall heating magnifies the adverse interaction effect on C_f and hastens the occurrence of incipient separation under the shock, whereas wall cooling has the opposite beneficial effect; it appears that proper T_w/T_t simulation may be of comparable importance to Re_L as regards skin friction.

Turning to the role of γ, it was found to have only a barely-discernable effect on the wall pressure distribution and displacement thickness over a wide range of Mach and

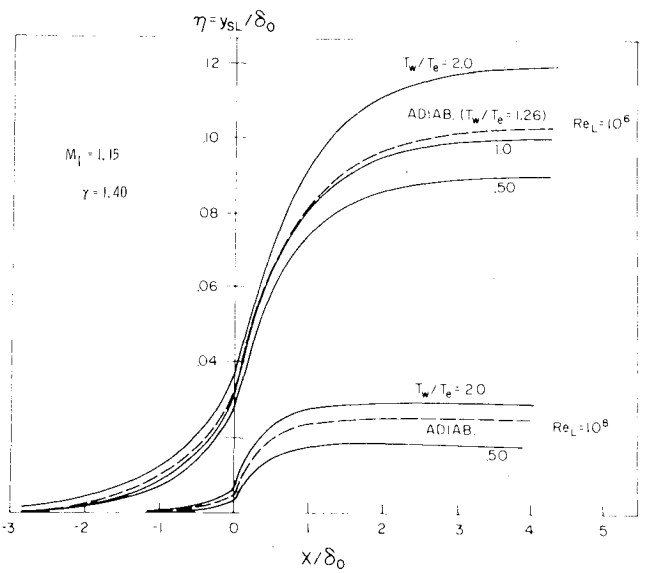

Fig. 3 Wall temperature effect on interactive thickening of the boundary layer.

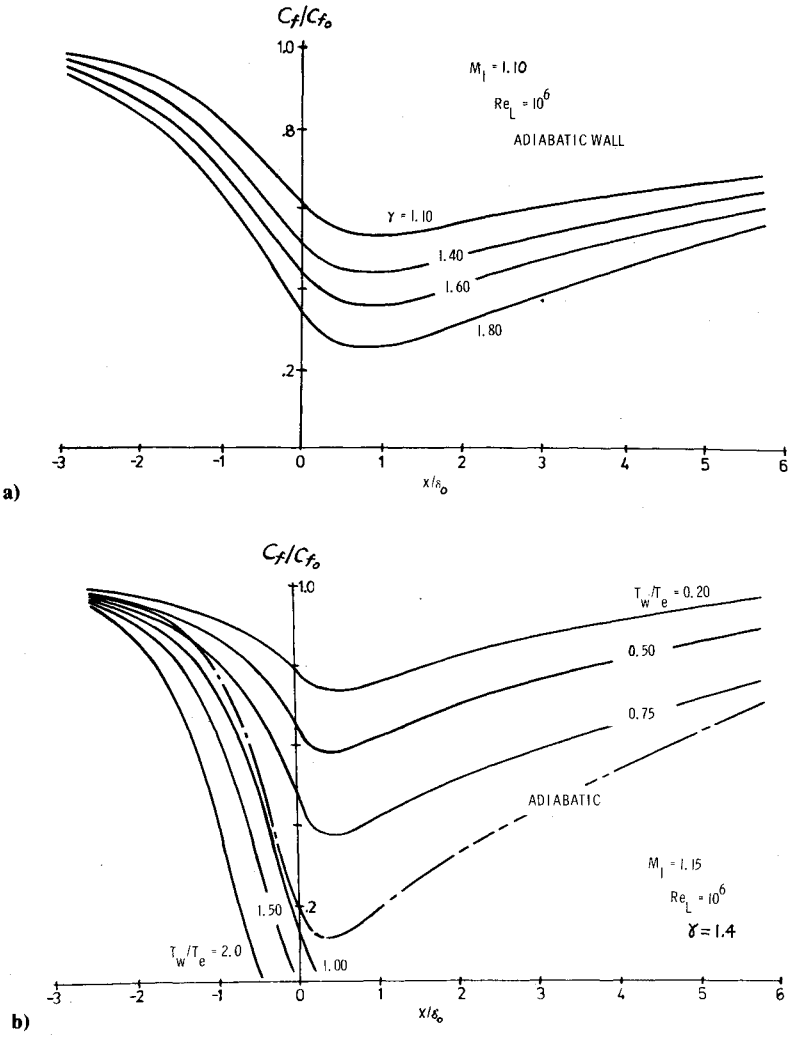

Fig. 4 Skin friction distributions through nonadiabatic real gas interaction: a) wall temperature effect; b) specific heat ratio effect.

Reynolds numbers, in agreement with experiment[3] and with laminar oblique interaction theory.[11] The typical influence on C_f, however, is more interesting as shown in Fig. 4b: increasing γ reduces C_f and moderately hastens the onset of incipient separation. This is explained by the increase of T_t with γ, which is qualitatively equivalent to a higher T_w.

Change in ω and Pr had a negligible effect on the interaction including skin friction.

Concluding Remarks

The present study results suggest that the combined lack of freeflight adiabatic wall temperature ratio and gas property simulation in a cryogenic tunnel can significantly exaggerate transonic shock-boundary layer interaction effects and attendant local separation on the model, compared to a flight case at the same M_1 and Re_L. Moreover, these similitude parameters also may have an indirect effect throughout the upstream boundary-layer history (as reflected by the incoming boundary-layer profile shape) because of the well-known sensitivity of shock-boundary-layer interaction to laminar-turbulent transition and streamwise pressure gradient history ahead of the shock, both of which can be influenced by T_w/T_t and γ. Thus, when interactive skin friction and incipient separation effects on wing aerodynamics are deemed important, these nonadiabatic real gas effects should be taken into account and may warrant further experimental as well as theoretical study. Moreover, we note two other practical applications of the present study: 1) post-entry transonic flight of the Space Shuttle orbiter, where transonic shock-boundary-layer interactions occur on an entry-heated surface history, and 2) transonic flows around cooled turbine blades operating in hot gas flows.

Acknowledgments

This work was supported by the Office of Naval Research under Contract N00014-75-C-0456. Helpful discussions with B. Kilgore and J. Adcock of NASA Langley are also gratefully acknowledged.

References

[1]Kilgore, R.A., Goodyer, M.J., Adcock, J.B. and Davenport, E.E., "The Cryogenic Wind Tunnel Concept for High Reynolds Number Testing," NASA TND-7762, 1974.

[2]Adcock, J.B., "Real Gas Effects Associated with One-Dimensional Transonic Flow at Cryogenic Nitrogen," NASA TND-8274, Dec. 1976.

[3]Gross, A.J. and Steinle, F.W., "Pressure Data from a 64A010 Airfoil at Transonic Speeds in Heavy Gas Media," NASA TM-62-468, Aug. 1975.

[4]Lighthill, M.J., "On Boundary Layers and Upstream Influence; II. Supersonic Flow Without Separation," *Proceedings of the Royal Society, A217*, 1953, pp. 478-507.

[5]Stratford, B.S., "The Prediction of Separation of the Turbulent Boundary Layer," *Journal of Fluid Mechanics*, pp. 1-16, 1959.

[6]Inger, G.R., "Upstream Influence in Interacting Non-Separated Turbulent Boundary Layers," Paper presented at the Workshop on Viscous Interaction and Boundary Layer Separation, Ohio State University, Columbus, Ohio, Aug. 17, 1976, VPI&SU Rept. Aero-090, Dec. 1978.

[7]Inger, G.R. and Mason, W.H., "Analytical Study of Transonic Normal Shock-Boundary Layer Interaction," *AIAA Journal*, Vol. 14, Sept. 1976, pp. 1266-72.

[8]Inger, G.R., "Theoretical Study of Reynolds Number and Mass Transfer Effects on Normal Shock-Turbulent Boundary Layer Interaction," *Zeitschrift für Luftund-Raufahrt Wissenshaften,* Band 2, Nov.-Dec. 1978.

[9]Inger, G.R., "Analysis of Transonic Shock with Nonadiabatic Turbulent Boundary Layers," presented as Paper 76-463 at the AIAA 11th Thermophysics Conference, San Diego, Calif., July 14-16, 1976.

[10]Inger, G.R., "On the Simulation of Transonic Shock-Turbulent Boundary Layer Interactions in Cryogenic or Heavy Gas Wind Tunnels," VPI&SU Report Aero-080, Blacksburg, Va., April 1978.

[11]Wagner, B. and Schmidt, W., "Theoretical Investigations of Real Gas Effects in Cryogenic Wind Tunnels," *AIAA Journal,* Vol. 16, June 1978, pp. 580-586.

Minimum Landing-Approach Distance for a Sailplane

Bion L. Pierson* and Imao Chen‡
Iowa State University, Ames, Iowa

Introduction

BECAUSE of the extremely low drag associated with modern high-performance sailplanes, the landing approach trajectory can become critical if aerodynamic deceleration devices are not used.[1] For the problem treated here, it is assumed that the sailplane approaches the landing strip head-on in still air with too much speed, altitude, or both to allow a conventional approach glide. It is also assumed that the initial altitude is too low for any kind of go-around maneuver. The problem can then be formulated as an optimal control problem, in which one seeks the lift coefficient time history which provides the shortest possible landing-approach distance. Alternately, the problem is one of transferring the sailplane from a prescribed initial state to a prescribed terminal state in a minimum distance. Furthermore, the flight is confined to a vertical plane. Sideslip or other lateral maneuvers are not allowed. The landing approach must also be made without benefit of spoilers, drag brakes, drag chutes, or other deceleration controls. Rotation (pitch) dynamics are neglected. Finally, it is necessary to impose minimum speed and altitude path constraints on the problem.

Problem Statement

Since the final time t_f is not specified, a control parameter, $\alpha = t_f$, is introduced via the time transformation

$$t = \alpha\tau \qquad 0 \le t \le t_f \qquad 0 \le \tau \le 1 \tag{1}$$

Thus, the variable end time problem will be transformed into a fixed end time problem with independent variable τ.

The point mass equations of motion are written with respect to the usual wind or trajectory axes.[2] Since the final range is to be minimized and since the range variable does not appear in the other dynamic equations, the range equation is simply incorporated into the performance index and is not required as part of the optimization process. The three remaining state variables are speed v, flight path angle γ, and altitude h.

The optimal control problem can be formally stated in terms of nondimensional variables as follows: Find the control function $u(\tau)$, $0 \le \tau \le 1$ and the control parameter α which minimize the performance index

$$J = \alpha \int_0^1 v \cos\gamma \, d\tau + k_1^{-1} \int_0^1 \left[(gX)^{1/2} \frac{v}{18} - 1 \right]^{-1} d\tau + k_2^{-1} \int_0^1 h^{-1} d\tau \tag{2}$$

subject to the dynamic constraints

$$\dot{v} = -\alpha[\eta C_D(u) v^2 + \sin\gamma] \qquad v(0) = 25(gX)^{-1/2} \tag{3a}$$

$$\dot{\gamma} = \alpha[\eta C_L(u) v^2 - \cos\gamma]/v \qquad \gamma(0) = -0.02 \text{rad} \tag{3b}$$

$$\dot{h} = \alpha v \sin\gamma \qquad h(0) = 50/X \tag{3c}$$

and subject to the terminal state constraints

$$v(1) = 23(gX)^{-1/2} \tag{4a}$$

$$\gamma(1) = 0 \tag{4b}$$

$$h(1) = 5/X \tag{4c}$$

where

$$C_D(u) = 0.018556 - 0.009652 C_L + 0.022288 C_L^2 \tag{5}$$

$$C_L(u) = C_{L_{\max.}} (2\sin^2 u - 1) \tag{6}$$

and

$$\eta = \tfrac{1}{2}\rho g X / (mg/S) = 0.01916015625 X \tag{7}$$

Note that a quadratic drag polar, Eq. (5), has been adopted. The coefficients correspond to a hypothetical medium-performance sailplane with maximum lift-to-drag ratio slightly in excess of 32. Also, note that the use of the transformation, Eq. (6), insures a lift coefficient with magnitude less than $C_{L_{\max.}} = 1.671$. From the boundary conditions in Eqs. (3) and (4), observe that the landing approach begins at an altitude of 50 m and a speed of 25 m/s and terminates at an altitude of 5 m and a speed of 23 m/s. Here, $X = 1000$ m is an arbitrary characteristic length used in the nondimensionalization, and $g = 9.81$ m/s^2 is the acceleration of gravity. In Eq. (3), the dot notation implies a derivative with respect to τ.

The second and third terms of the performance index, Eq. (2), represent integral interior penalty functions[3] for the speed and altitude path constraints, respectively. The second term limits the speed to values above the stall speed of 18 m/s. The third term enforces positive altitudes. As with any penalty function scheme, it is necessary to solve a sequence of unconstrained subproblems, Eqs. (2-7), with fixed positive penalty constants k_1 and k_2. These penalty constants are then increased between successive subproblems to allow the solution point to move closer to the active constraint surfaces. With the use of these interior penalty functions, it is necessary to begin computations with a nominal control which generates a trajectory satisfying both state inequality constraints.

Received Aug. 31, 1978; revision received Nov. 30, 1978.

Index categories: Landing Dynamics; Performance; Guidance and Control.

*Professor, Department of Aerospace Engineering and the Engineering Research Institute. Member AIAA.

†Graduate Student, Department of Aerospace Engineering.